Analytical Biochemistry 408 (2011) 136–146

Contents lists available at ScienceDirect

Analytical Biochemistry

journal homepage: www.elsevier.com/locate/yabio

Label-free liquid chromatography–tandem mass spectrometry analysis with automated phosphopeptide enrichment reveals dynamic human milk protein phosphorylation during lactation

John W. Froehlich [a], Caroline S. Chu [a], Ning Tang [b], Keith Waddell [b], Rudolf Grimm [b], Carlito B. Lebrilla [a,c,*]

[a] Department of Chemistry, University of California, Davis, Davis, CA 95616, USA
[b] Agilent Technologies, Santa Clara, CA 95051, USA
[c] Department of Biochemistry and Molecular Medicine, University of California, Davis, Davis, CA 95616, USA

ARTICLE INFO

Article history:
Received 16 July 2010
Received in revised form 7 August 2010
Accepted 25 August 2010
Available online 17 September 2010

Keywords:
Milk
Phosphoprotein
Quantification
Label free
Proteomics

ABSTRACT

Protein phosphorylation is a critical posttranslational modification that affects cell–cell signaling and protein function. However, quantifying the relative site-specific changes of phosphorylation occupancies remains a major issue. An online enrichment of phosphopeptides using titanium dioxide incorporated in a microchip liquid chromatography device was used to analyze trypsin-digested human milk proteins with mass spectrometry. The method was validated with standards and used to determine the dynamic behavior of protein phosphorylation in human milk from the first month of lactation. α-Casein, β-casein, osteopontin, and chordin-like protein 2 phosphoproteins were shown to vary during this lactation time in an independent manner. In addition, changes in specific regions of these phosphoproteins were found to vary independently. Novel phosphorylation sites were discovered for chordin-like protein 2, α-lactalbumin, β-1,4-galactosyl transferase, and poly-Ig (immunoglobulin) receptor. Coefficients of variation for the quantitation were comparable to those in other contemporary approaches using isotopically labeled peptides, with a median value of 11% for all phosphopeptide occupancies quantified.

Phosphorylation, which has been shown to affect protein function and cell–cell signaling, is a widespread and critical post-translational modification (PTM).[1] Determination of protein phosphorylation by mass spectrometry is challenging for a number of reasons, a few of which include the relative lability of the phosphate group, substoichiometric quantities of the PTM, and ion suppression of phosphopeptides in the presence of peptides that are also generated by sample preparation. There have been a number of solutions to the second and third of these challenges that mainly use chromatographic enrichment of phosphopeptides. Phosphopeptide or phosphoprotein enrichment has been achieved through immobilized metal affinity chromatography, strong cation or anion exchange chromatography, titanium dioxide enrichment, and antibodies. Recently, a chip-based platform has been developed for automated phosphopeptide enrichment and analysis by nano-liquid chromatography–tandem mass spectrometry (nLC–MS/MS) [1]. This platform combines the advantages of selective, reproducible, automated phosphopeptide enrichment with an integrated MS nanospray emitter that may be directly coupled to a variety of instruments. The current study uses this platform for the analysis of human milk phosphorylation during the first month of lactation.

An extensive abundance of glycosylated and phosphorylated milk proteins and a high abundance of the completely indigestible human milk oligosaccharides (HMOs) combine to suggest that milk is much more than a nutrition source. Indeed, HMOs have been shown to possess a variety of biological roles, including selection of a healthy microbiota and functioning as receptor analogues for pathogenic bacteria [2]. Similarly, the protein fraction of human milk possesses a wide variety of bioactivities, including immunomodulatory, bacteriostatic, bacteriocidal, anti-inflammatory, and apoptotic activities [3]. Human milk proteins also exhibit proteolytic [4] and lipolytic [5] activities. In addition, many milk proteins are resistant to digestion. This resistance, in concert with a developing neonatal digestive system, facilitates the survival of both fully intact and minimally degraded biologically active forms of milk proteins in the gastrointestinal tract (GIT) of the infant [6].

* Corresponding author at: Department of Biochemistry and Molecular Medicine, University of California, Davis, Davis, CA 95616, USA.
E-mail address: cblebrilla@ucdavis.edu (C.B. Lebrilla).

[1] *Abbreviations used:* PTM, posttranslational modification; nLC–MS/MS, nano-liquid chromatography–tandem mass spectrometry; HMO, human milk oligosaccharide; GIT, gastrointestinal tract; OPN, osteopontin; CHRDL2, chordin-like protein 2; HPLC, high-performance liquid chromatography; BSA, bovine serum albumin; TOF, time-of-flight; CV, coefficient of variation; NPA, normalized phosphopeptide area; Ig, immunoglobulin; CID, collision-induced dissociation; EIC, extracted ion chromatogram; MGCK, mammary gland casein kinase.

0003-2697/$ - see front matter © 2010 Elsevier Inc. All rights reserved.
doi:10.1016/j.ab.2010.08.031

These phenomena demonstrate that although the protein fraction of human milk presents a near perfect dietary balance of amino acids, it is by no means merely a source of amino acids. Instead, the emerging view is that milk is a highly functional food [7] that influences bacterial colonization [8], attunes neonatal immune response [9], and promotes infant brain development [10] via specific components present in the mixture. Quantitative changes in these specific components during lactation likely cause a change in the bioactivities that milk provides.

In fact, quantitative variations of these specific components during lactation could be driven by the development of the neonate. In particular, the nutritional needs, intestinal flora, and immune system of the neonate change as he or she grows. Milk has been shown to modulate each of these; for example, the neonate's need for supplementary support of his or her immune system also diminishes as the neonate grows. Although the mother could potentially continue to express and secrete these immunological factors into milk after the neonate's own immune system has developed, this would represent a substantial physiological inefficiency. Instead, it appears that the abundance of these components decreases as the need for them decreases. Similar changes for specific PTMs such as phosphorylation could also lend insight to what biological roles the PTMs support. The determination of quantitative changes in milk protein phosphorylation in this study is performed with these considerations in mind.

The majority of milk protein phosphorylation is present in a class of proteins known as caseins. In human milk from the first month of lactation, phosphorylated α- and β-casein comprise approximately 10 to 30% of the total protein present [11]. κ-Casein is extensively glycosylated and constitutes the remainder of the casein fraction. The caseins are critical to mineral transport and absorption within the infant's digestive system, and they complex with calcium phosphate to form the micelles present in milk. The phosphorylation sites of the caseins have been extensively characterized [12–14], and further site determination of these well-studied phosphoproteins is not the goal here. In the current study, a label-free method was developed to determine the changes in phosphorylation site occupancy during the first month of lactation. Quantitative changes in phosphorylation site occupancy for four milk phosphoproteins are reported: α-casein, β-casein, osteopontin (OPN), and chordin-like protein 2 (CHRDL2).

Materials and methods

Materials

All water used was generated by Milli-Q filtration and was measured as 18 MΩ water. The phosphopeptide kit, containing the phosphochip and necessary elution and regeneration solutions, was provided by Agilent Technologies (Santa Clara, CA, USA). Sequencing-grade modified trypsin was purchased from Promega (Madison, WI, USA). Formic acid (high-performance liquid chromatography [HPLC] grade), acetic acid (HPLC grade), dithiothreitol, iodoacetamide, and Tris buffer all were purchased from Sigma–Aldrich (St. Louis, MO, USA). Acetonitrile (Honeywell Burdick & Jackson) was purchased from VWR (West Chester, PA, USA).

Samples

Samples were donated by a healthy individual donor. Milk was collected by manual expression and immediately frozen at −80 °C until ready for protein extraction. A thawed aliquot (250 μl) of milk from a single donor from lactation days 2, 5, 10, 17, and 29 was adjusted to 1 mM sodium orthovanadate and skimmed by centrifugation at 4 °C for 30 min. Skimmed milk was dialyzed against a solution of 25 mM NH_4HCO_3 and 1 mM sodium orthovanadate (pH 7.4) for 16 h with two changes of dialysate.

Bulk sample protein quantitation

Dialyzed milk samples were quantified via the Bradford method using bovine serum albumin (BSA) for the calibration curve.

Protein digestion

Aliquots of 200 μg of each sample were used for proteolysis. Samples were reduced with 3 μl of 0.5 M dithiothreitol at 55 °C for 45 min. Alkylation was performed by the addition of 6 μl of 450 mM iodoacetamide, followed by incubation in the dark at room temperature for 20 min. Samples were desalted using C_{18} cartridges and dried in vacuo.nLC–MS/MS conditions and phosphopeptide enrichment.

Samples were reconstituted in 3% acetonitrile and analyzed using an Agilent 1200 series microwell plate autosampler (maintained at 6 °C), capillary pump, nanopump, HPLC–chip interface, and the Agilent 6520 qTOF (quantitative time-of-flight) LC–MS/MS system. The Phosphochip (G4240-62021) consists of a 40-nl "sandwiched" C_{18}–TiO_2–C_{18} enrichment column and a 43 × 0.075-mm (i.d.), 5-μm C_{18} analytical column. For sample loading, the capillary pump delivered 0.1% formic acid in 3.0% acetonitrile in water (v/v) isocratically at 3 μl/min. The injection volume was 15 μl for each sample. Technical triplicates were injected. A gradient was delivered at 0.3 μl/min using 0.5% formic acid and 0.6% acetic acid in 3% acetonitrile in water (v/v) (A) and 0.5% formic acid and 0.6% acetic acid in 90% acetonitrile in water (v/v) (B). A 60-min nLC gradient was run from 0 to 35% B, 0 to 40 min; 35 to 45% B, 40 to 45 min; 45 to 90% B, 45 to 48 min; and held for 2 min at 100% B with an equilibration time of 10 min at 0% B. The drying gas temperature was set at 325 °C with a flow of 4.0 L/min (2.0 L of nitrogen and 2.0 L of dry-grade compressed air). Precursor scan data were acquired in the positive ionization mode within a mass range of m/z 300 to 2000. Tandem mass spectra were acquired from m/z 50 to 3000. Variable collision voltages of −4.8 +3.6 V/100 m/z were used for fragmentation. Mass correction was enabled for all precursor scan data using a reference mass of m/z 1221.991, an internal standard (electrospray ionization [ESI]–TOF Tuning Mix G1969-85000, Agilent Technologies). Data analysis was performed using Spectrum Mill, MassHunter Qualitative Analysis Software B.01.03 Build 157, and Microsoft Excel 2007.

Database searching

Deconvolution, deisotoping, data extraction, and database searching were performed using Spectrum Mill. After data processing, the Swiss–Prot database (sp. *Homo sapiens*) was searched with the following parameters: peptide mass range of 400–4500 Da. Carbamidation of cysteine residues was included as a constant modification. In addition, deamidation of asparagines, oxidation of methionines, and phosphorylation of serine, threonine, and tyrosine residues were also searched as variable modifications.

Peptide and protein validation

Peptides were validated in an automated fashion using Spectrum Mill. Charge states of 5, 4, 3, and 2 were allowed, requiring scores of 10, 9, 8, and 7, respectively. All peptides also required a delta forward–reverse score of at least 3, and a minimum of 65% of the intensity of MS/MS spectra was required to be assigned for the assignment to be validated. Peptide and phosphopeptide MS/MS spectra were automatically validated as above. Phosphopeptide

assignments were also manually verified by inspection to determine the accuracy of the automated phosphorylation site assignments.

Protein identifications were also validated in an automated fashion. All proteins with a Spectrum Mill score above 25 and with at least two unique peptides were considered as valid in this study.

Table 1
Summary of proteins identified via nLC–MS/MS analyses.

Protein name	Accession number	% AA coverage	Number of unique peptides	Score
Lactotransferrin	P02788	88	91	1896
Serum albumin	P02768	85	68	1215
Polymeric immunoglobulin receptor	P01833	**52**	**48**	**879**
Bile salt-activated lipase	P19835	46	40	745
Xanthine dehydrogenase/oxidase	P47989	31	35	604
Alpha-lactalbumin	**P00709**	**51**	**19**	**403**
Ig alpha-1 chain C region	P01876	76	19	387
Clusterin	P10909	34	17	296
Osteopontin	P10451	**57**	**17**	**255**
Immunoglobulin J chain	P01591	78	13	250
Chordin-like protein 2	**Q6WN34**	**41**	**13**	**248**
Alpha-S1-casein OS	**P47710**	**58**	**13**	**244**
Leucine-rich alpha-2-glycoprotein	P02750	46	13	242
Adipophilin	Q99541	43	14	242
Butyrophilin subfamily 1 member A1	Q13410	32	15	234
Alpha-1-antitrypsin	P01009	32	13	232
Fatty acid-binding protein, heart	P05413	83	13	232
Monocyte differentiation antigen CD14	P08571	48	13	217
Ig lambda chain C regions	P01842	97	11	208
Lactadherin	Q08431	42	12	204
Beta-casein	**P05814**	**82**	**11**	**203**
Kappa-casein	P07498	56	11	198
Ig kappa chain C region	P01834	89	9	193
Apolipoprotein A-I	P02647	50	13	187
Serotransferrin	P02787	22	12	185
Zinc-alpha-2-glycoprotein	P25311	37	9	166
Haptoglobin	P00738	30	9	160
Macrophage mannose receptor 1-like protein 1	Q5VSK2	7	10	145
Ig mu chain C region	P01871	28	9	142
Tenascin	P24821	6	8	137
Alpha-1-antichymotrypsin	P01011	18	9	134
Fatty acid synthase	P49327	4	8	124
Beta-1,4-galactosyltransferase 1	**P15291**	**30**	**7**	**122**
Complement C4-B	P0C0L5	8	8	119
Alpha-1-acid glycoprotein 1	P02763	25	5	96
Lipoprotein lipase	P06858	22	6	91
Actin, cytoplasmic 2	P63261	24	6	90
Mucin-4	Q99102	2	5	88
Lysozyme C	P61626	43	5	87
Alpha-enolase	P06733	20	6	84
Ig gamma-1 chain C region	P01857	21	4	81
Beta-2-microglobulin	P61769	37	4	65
Ig kappa chain V-III region GOL	P04206	36	3	58
Complement C3	P01024	2	3	57
Alpha-lB-glycoprotein	P042l7	9	3	46
Galectin-3-binding protein	Q08380	7	3	40
Peptidyl-prolyl cis-trans isomerase A	P62937	15	2	39
Sulfhydryl oxidase l	O00391	4	2	38
Ig lambda chain V-III region LOI	P80748	21	2	37
Ig kappa chain V-I region WEA	P0l6l0	21	2	35
RBl-inducible coiled-coil protein l	Q8TDY2	0	3	35
Mucin-l	P15941	1	2	34
Ig heavy chain V-III region BRO	P0l766	19	2	32
Apolipoprotein A-II	P02652	42	2	32
Proactivator polypeptide	P07602	4	2	31
Ig heavy chain V-III region WAS	P01776	19	2	30
Ubiquitin	P62988	27	2	30
UTP-glucose-l-phosphate uridylyltransferase	Q16851	4	2	28
Myosin-VI	Q9UM54	3	3	27
Insulin-like growth factor-binding protein 2	P18065	10	2	26
Ig lambda chain V-I region WAH	P04208	16	2	26
Sclerostin domain-containing protein l	Q6X4U4	18	2	25
Nucleobindin-2	P80303	7	2	23
Selenium-binding protein l	Q13228	4	2	21
Uncharacterized protein KIAA0467	Q5T011	0	2	21
Ig heavy chain V-III region GAL	P01781	13	2	20

Note. Protein name, accession number, percentage amino acid (AA) coverage, and number of unique peptides are annotated. Phosphoproteins identified in this study are in bold.

Table 2
Summary of the 44 unique phosphopeptides quantified in these studies.

Protein name	Number of phosphates	Swiss-Prot	Variations of site	Peptide sequence	RT	*m/z*	Score	Fold-change	Significance level	Maximum day	Minimum Day	D2 mean	D2 RSD	D5 mean	D5 RSD	D10 mean	D10 RSD	D17 mean	D17 RSD	D29 mean	D29 RSD
ACAS	1	P47710		(K)MESSISSSSEEMSLSK(C)	23.46	600.2407	20.6	1.39	**	2	29	1.13E+06	7	9.77E+05	11	1.00E+06	8	8.70E+05	2	8.08E+05	6
ACAS	2	P47710		(K)MESSISSSSEEMSLSK(C)	23.83	939.841	15.5	1.49	***	2	29	4.50E+05	6	3.82E+05	11	3.65E+05	8	3.24E+05	5	3.02E+05	4
ACAS	1	P47710	M –>m	(K)MESSISSSSEEMSLSK(C)	20.56	907.8385	19.0	1.73	***	2	17	3.30E+05	8	2.66E+05	11	2.33E+05	8	1.91E+05	3	2.27E+05	3
ACAS	1	P47710	M –>m	(K)MESSISSSSEEMSLSK(C)	21.81	907.8508	20.9	1.33	**	2	17	7.43E+05	7	6.93E+05	11	6.12E+05	7	5.57E+05	4	5.92E+05	5
ACAS	1	P47710	M –>m	(K)MESSISSSSEEMSLSK(C)	23.34	605.5716	21.1	1.47	*	5	17	2.83E+05	11	2.92E+05	20	2.54E+05	12	1.99E+05	9	2.00E+05	21
ACAS	1	P47710	**41**	**(R)LQNPSESSEPIPLEsR(E)**	25.87	621.6178	19.1	1.41	*	2	29	3.42E+07	13	2.88E+07	18	2.95E+07	10	2.61E+07	6	2.44E+07	15
ACAS	1	P47710	**33**	**(R)LQNPSEsSEPIPLESR(E)**	26.43	621.6116	23.2	2.35	**	5	2	9.34E+06	15	2.19E+07	15	1.55E+07	13	1.41E+07	4	1.30E+07	15
ACAS	2	P47710		(R)LQNPSESSEPIPLESR(E)	26.67	971.897	20.4	1.46	*	29	5	1.98E+07	16	1.52E+07	27	1.65E+07	20	2.02E+07	5	2.23E+07	9
ACAS	3	P47710	**31,33,41**	**(R)LQNPsEsSEPIPLEsR(E)**	26.68	1011.8905	12.9	1.34	**	29	10	9.28E+05	8	8.92E+05	14	8.33E+05	8	1.03E+06	7	1.12E+06	4
BCAS	1	P05814		(R)ETIESLSSSEESITEYK(Q)	28.06	671.2771	12.4	2.71	**	29	10	2.26E+05	17	2.47E+05	20	2.16E+05	15	3.02E+05	22	5.85E+05	28
BCAS	1	P05814	**25**	**(R)ETIESLSSsEESITEYK(Q)**	29.81	1006.4277	13.8	3.06	**	29	5	3.22E+05	16	3.04E+05	18	3.76E+05	17	8.54E+05	19	9.32E+05	20
BCAS	2	P05814	**24,25**	**(R)ETIESLSssEESITEYK(Q)**	28.86	1046.3926	19.3	3.11	**	17	5	1.04E+06	16	5.58E+05	18	1.17E+06	17	1.74E+06	20	1.46E+06	20
CHRDL2	1	4 Q6WN3	**182**	**(K)DEASEQsDEEDSVQSLHGVR(H)**	21.63	766.29	23.1	2.51	**	2	17	2.18E+06	19	9.85E+05	37	1.29E+06	39	8.70E+05	19	1.53E+06	24
				(K)DEASEQsDEEDSVQSLHGVRHPQD																	
CHRDL2	1	4	**182**	**PCSSDAGR(K)**	20.43	901.8612	12.2	2.67	**	2	17	4.59E+05	18	2.31E+05	37	2.96E+05	39	1.72E+05	19	3.45E+05	24
CHRDL2	2	4 Q6WN	**179,182**	**(K)DEAsEQsDEEDSVQSLHGVR(H)**	22.45	792.964	13.4	2.19	**	2	5	2.64E+05	17	1.21E+05	35	1.85E+05	39	1.34E+05	19	2.15E+05	29
				(K)DEAsEQsDEEDSVQSLHGVRHPQD																	
CHRDL2	2	4	**179,182**	**PCSSDAGR(K)**	21.05	737.6853	15.8	2.24	**	2	17	2.43E+05	18	1.32E+05	36	1.77E+05	39	1.09E+05	19	2.06E+05	30
OST	2	P10451	**62,63**	**(K)QNLLAPQNAVssEETNDFK(Q)**	29.79	1132.956	12.2	3.54	***	29	5	1.05E+05	19	8.91E+04	41	1.34E+05	20	2.83E+05	6	3.15E+05	6
				(K)QNLLAPQNAVssEETNDFKQETLPS																	
OST	2	P10451		K(S)	30.22	1016.7695	13.1	1.74	***	2	5	1.40E+05	7	8.05E+04	6	9.43E+04	8	9.54E+04	7	8.30E+04	5
				(R)RPDIQYPDATDEDITsHMESEELNGA																	
OST	1	P10451		YK(A) (R)RPDIQYPDAtDEDITsHMESEELNGA	30.37	826.8363	15.2	2.15	***	2	17	4.81E+06	11	2.23E+06	8	3.60E+06	9	2.23E+06	5	2.71E+06	5
OST	2	P10451		YK(A) (R)RPDIQYPDAtDEDITsHMESEELNGA	30.58	846.827	10.4	2.01	***	2	5	1.47E+06	5	7.32E+05	14	1.16E+06	4	1.07E+06	6	1.28E+06	6
OST	2	P10451		YK(A) (R)RPDIQYPDAtDEDITsHMEsEELNGA	31.70	846.827	16.7	3.90	***	17	5	1.66E+06	4	7.15E+05	9	2.71E+06	12	2.79E+06	8	1.97E+06	6
OST	3	P10451		YK(A)	31.76	866.8169	15.6	7.42	***	17	5	7.34E+05	4	2.42E+05	6	1.19E+06	13	1.79E+06	5	9.46E+05	11
OST	1	P10451		(K)AIPVAQDLNAPsDWDSRGK(D)	29.22	707.3255	12.2	1.88	**	5	17	2.71E+06	15	3.80E+06	7	2.93E+06	3	2.02E+06	5	3.26E+06	8
OST	1	P10451	**219**	**(K)AIPVAQDLNAPSDWDsR(G)**	31.27	967.9333	23.1	1.96	***	10	29	1.71E+07	9	1.48E+07	16	1.99E+07	15	1.40E+07	9	1.02E+07	7
OST	2	P10451		(K)AIPVAQDLNAPsDWDsR(G)	31.98	1007.8992	8.2	5.38		10	2	2.60E+04	39	3.49E+04	20	1.40E+05	10	7.87E+04	20	6.84E+04	22
OST	2	P10451		(R)GKDsYETSQLDDQsAETHSHK(Q)	16.05	631.4949	9.1	1.30	~	29	17	7.09E+05	9	5.57E+05	8	5.77E+05	8	5.49E+05	6	7.11E+05	19
OST	2	P10451		(R)GKDSYETsQLDDQsAETHSHKQSR(L)	15.07	724.2851	18.5	1.59	**	2	17	1.55E+06	7	1.05E+06	12	1.26E+06	17	9.77E+05	14	1.46E+06	6
OST	3	P10451		(K)AIPVAQDLNAPsDWDsRGKDsYETS	28.92	888.5433	13.8	1.96	*	10	29	3.81E+06	9	2.47E+06	19	4.19E+06	22	3.42E+06	13	2.14E+06	17
				QLDDQSAETHSHK(Q)																	
OST	1	P10451	**263**	**(K)ANDESNEHSDVIDSQELsK(V)**	20.09	732.9663	20.2	2.09	***	5	17	2.27E+05	8	4.25E+05	10	3.11E+05	9	2.03E+05	5	3.70E+05	8
OST	1	P10451	**254**	**(K)ANDEsNEHSDVIDSQELSK(V)**	20.74	732.9626	18.4	2.03	***	5	17	4.56E+05	5	7.19E+05	7	5.29E+05	4	3.54E+05	5	6.59E+05	7
OST	2	P10451		(K)ANDEsNEHSDVIDsQELSK(V)	21.04	759.6217	19.6	1.35	***	10	17	2.35E+06	3	2.14E+06	6	2.38E+06	3	1.77E+06	4	2.32E+06	5
OST	1	P10451	**254**	(R)KANDESNEHsDVIDSQELSK(V)	19.28	581.9981	10.7	3.09	–	29	2	2.61E+04	66	4.12E+04	82	5.56E+04	120	5.00E+04	80	8.07E+04	93
OST	2	P10451	**254, 263**	**(R)KANDESNEHsDVIDSQELsK(V)**	19.67	802.3174	15.0	1.58	–	29	5	1.40E+06	49	1.24E+06	63	1.60E+06	58	1.48E+06	48	1.96E+06	38
OST	3	P10451	**254, 258, 263**	**(R)KANDEsNEHsDVIDsQELSK(V)**	19.85	828.9763	10.9	3.01	***	29	2	1.57E+05	24	2.28E+05	31	3.43E+05	30	3.44E+05	21	4.72E+05	9
OST	2	P10451	**M –>m 275, 280**	**(R)EFHsHEFHsHEDmLVVDPK(S)**	22.11	624.7453	10.5	2.49	***	29	17	3.58E+06	3	4.13E+06	7	2.81E+06	8	2.11E+06	5	5.24E+06	6
OST	2	P10451	**275,280**	**(R)EFHsHEFHsHEDMLVVDPK(S)**	24.51	620.7382	9.6	1.46	***	2	17	6.44E+06	5	5.29E+06	6	4.91E+06	4	4.41E+06	5	5.74E+06	7
OST	1	P10451		(R)ISHELDsASSEVN(-)	18.03	734.3083	13.1	3.57	***	10	5	3.86E+04	20	1.23E+04	10	4.40E+04	5	3.41E+04	10	2.83E+04	24
OST	1	P10451		(R)IsHELDSASSEVN(-)	18.88	734.2938	15.1	4.20	–	29	17	2.22E+05	24	3.20E+05	26	1.37E+05	27	7.75E+04	33	3.25E+05	94
OST	2	P10451		(R)IsHELDSASsEVN(-)	18.81	774.2699	10.0	2.70	***	2	5	2.42E+05	3	8.96E+04	35	1.81E+05	20	1.50E+05	23	1.52E+05	81
OST	2	P10451		(R)IsHELDsASSEVN(-)	19.65	774.2817	9.9	3.02	**	2	17	2.41E+05	18	1.32E+05	73	1.53E+05	61	8.00E+04	51	2.24E+05	38
OST	1	P10451	**303**	**(K)FRISHELDSAsSEVN(-)**	26.73	590.928	14.2	5.32	***	29	17	6.36E+06	3	1.71E+07	9	6.42E+06	5	3.84E+06	8	2.04E+07	6
OST	2	P10451		(K)FRIsHELDsASSEVN(-)	25.66	925.8497	9.7	3.32	**	2	5	1.98E+05	15	5.96E+04	30	1.01E+05	18	7.32E+04	8	6.63E+04	8
OST	2	P10451	**303+(x)**	**(K)FRISHELDsASSEVN(-)**	26.64	925.8497	10.7	3.74	***	17	5	1.35E+06	20	6.48E+05	7	2.16E+06	9	2.43E+06	5	2.39E+06	12
OST	2	P10451	**303+(x)**	**(K)FRISHELDsASSEVN(-)**	27.51	925.8497	10.8	3.35	***	29	17	5.46E+06	6	7.15E+06	5	4.11E+06	4	2.35E+06	6	7.88E+06	10

Note. RT, retention time; D, day; RSD, relative standard deviation. All quantitative values are reported as the means of normalized triplicate analyses along with RSDs for lactation days. Two-tailed heteroscedastic *t* tests were performed, and the significance levels between the maximum and minimum quantitative values are also annotated. Singly, doubly, and triply marked (asterisks) entries correspond to significance levels of $P < 0.05$, $P < 0.01$, and $P < 0.001$, respectively.

Relative phosphorylation quantitation

A protein-specific normalization strategy was used as follows. First, all validated peptide signals for a given protein were summed, and triplicate technical replicates were used to calculate the standard deviations of the total peptide intensities for each individual phosphoprotein quantified in this study. A protein-specific normalization factor, *N*, was then generated as follows for each phosphoprotein at each lactation day:

$$N(\textit{phosphoprotein } x, \textit{day } y) = \frac{\textit{maximum}(\sum[\textit{peptide intensities}]\textit{all days})}{\sum[\textit{peptide intensities}]\textit{day } y}$$

After generating *N* values, all validated phosphopeptide MS/MS spectra were combined into a list. Phosphopeptides that were not validated in each sample were not selected for quantification. Precursor MS scans corresponding to the extracted ion chromatograms from the first four isotopic peaks (i.e., the monoisotopic mass and the $m + 1$, $m + 2$, and $m + 3$) of validated phosphopeptides were summed. These raw values were then multiplied by *N* to yield normalized abundances, and the errors of each measurement were propagated during this calculation to yield coefficients of variation (CVs). All quantitative comparisons are based on the normalized phosphopeptide areas (NPAs). The final measurements are

$$NPA = \frac{\sum_m^{m+3} ppArea}{N} \pm \sqrt{\left(CV\left(\sum_m^{m+3} ppArea\right)\right)^2 + (CV(N))^2}$$

where the first quotient gives the mean (reported value) and the second gives the CV.

Results

Validation of the experimental approach

To validate the quantification strategy outlined above, a standard containing equimolar amounts of a BSA standard and FQsEEQQQTEDELQDK phosphopeptide from bovine β-casein was used. First, varying amounts of the standard were injected, and a standard curve of the intensity of the FQsEEQQQTEDELQDK phosphopeptide versus the amount injected was calculated. This plot possessed a high linearity (see Supplementary Fig. 1 in supplementary material). The MS intensity of each peptide identified was summed for each point on the standard curve, and the ratio of total BSA peptide signal to total phosphopeptide signal was also determined for each point on the standard curve. The ratio of β-casein phosphopeptide response to peptide response remained approximately constant despite varying quantities injected, supporting the normalization approach used in this work.

Protein identification and phosphorylation site determination

All proteins identified in this study are listed in Table 1. Values for the total number of peptides identified, percentage sequence coverage, Spectrum Mill protein score, total peptide intensity for a given protein, and standard deviations of peptide intensity measurements for each protein are also annotated. Proteins identified as phosphorylated in this study are highlighted in the table. In total, 66 proteins and 7 phosphoproteins were identified. The abundant whey proteins lactoferrin, α-lactalbumin, and immunoglobulin A were well represented in the peptide nLC–MS fractions.

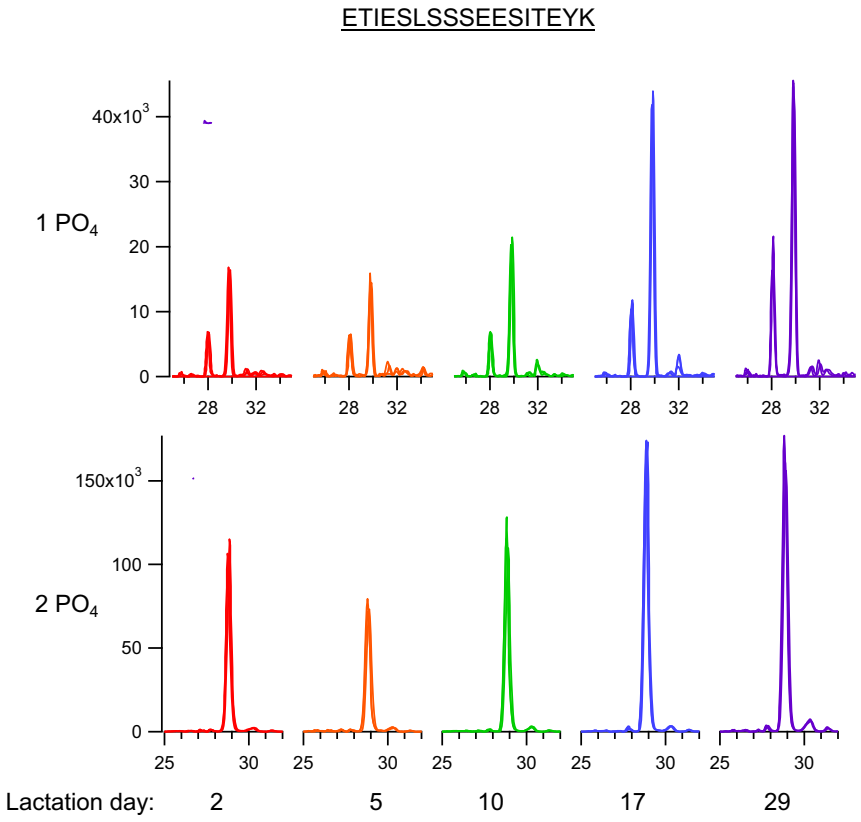

Fig.1. Overlaid triplicate EICs of monophosphorylated (upper) and diphosphorylated (lower) peptide ETIESLSSSEESITEYK from β-casein. Isomeric separation of the monophosphorylated peptide is observed. The more abundant peak eluting at 29.8 min corresponds to ETIESLSSsEESITEYK (pSer25). Only a single isomer of the diphosphorylated peptide is observed.

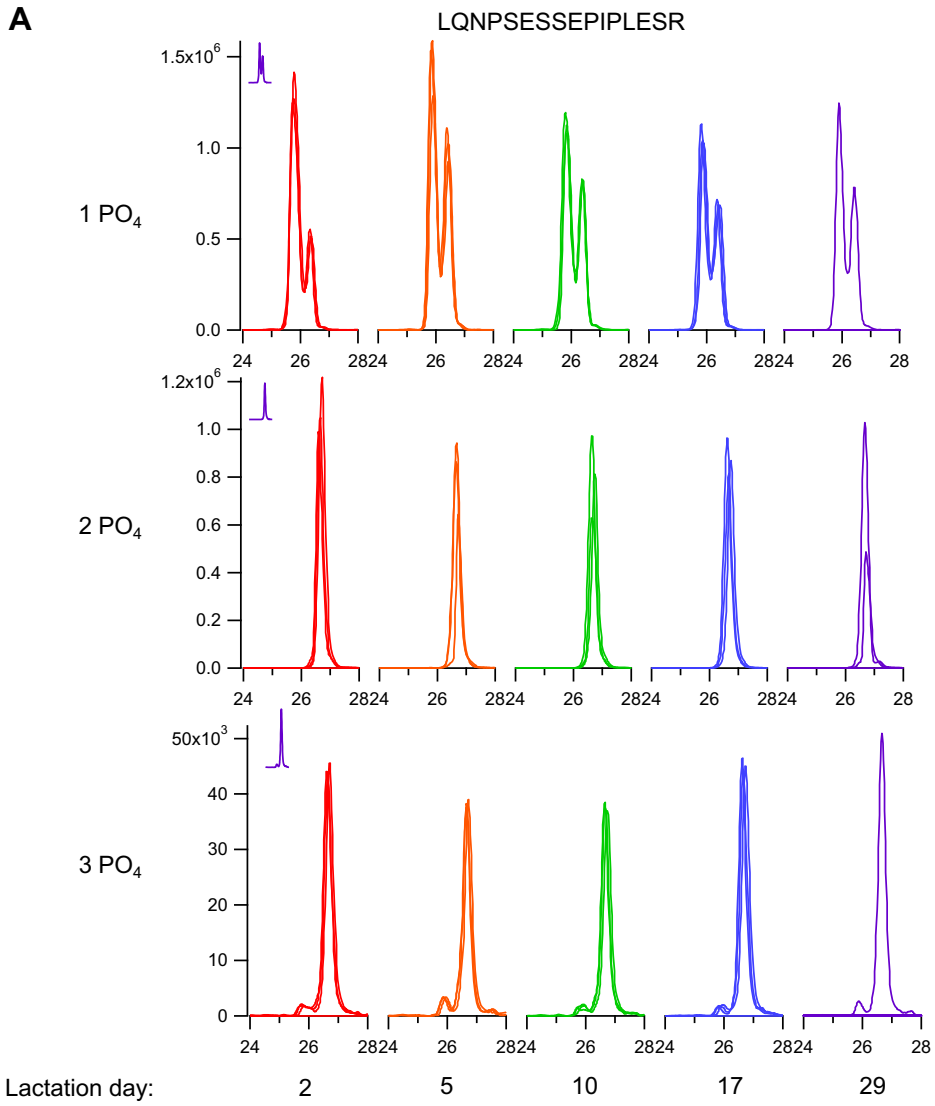

Fig.2. (A) Overlaid triplicate EICs of singly, doubly, and triply phosphorylated LQNPSESSEPIPLESR peptide from α-casein. Isomeric separation is apparent for the monophosphorylated peptide only. Minor, yet significant, differences are observed. The largest relative change occurs between days 2 and 5 of the monophosphorylated isomer eluting at 26.4 min, corresponding to LQNPSEsSEPIPLESR (pSer33), whereas the major species eluting at 25.9 min is LQNPSESSEPIPLEsR (pSer41).

As expected, OPN, α-casein, and β-casein were the most abundant proteins present in the phosphopeptide fractions.

Low amounts of phosphorylation were also detected in poly-Ig (immunoglobulin) receptor, β-1,4-galactosyltransferase, and α-lactalbumin; however, these phosphopeptides were not observed in all of the samples, and so any potential changes in abundance were not quantified. Notably, α-lactalbumin is not annotated as a phosphoprotein in the Swiss–Prot, PhosphoSite, or other databases, suggesting that this is the first report of its phosphorylation. CHRDL2 was also identified as phosphorylated, with two novel sites identified in this study. Only a single phosphorylation site on a single protein isoform was discovered previously [15].

Protein identification and phosphorylation site determination

To quantify changes in phosphorylation site occupancy of specific proteins in complex samples, changes in the protein quantities must first be considered. This was achieved via a label-free quantification method. Two commonly used schemes were compared to determine variation in phosphoprotein expression: spectral counting and total peptide intensity. Although spectral counts have been used to compare the relative quantities of different proteins, the goal of comparing a given protein between samples is better suited for a peak area-based quantitation strategy [16]. This approach will not allow the comparison of different proteins (i.e., the quantitation of α-casein to β-casein in different samples), but it has been shown to yield more reproducible and sensitive results for the relative quantitation of a given protein between samples [16]. On application of each method to our results, the peptide area-based quantitation was found to be both more reproducible and more sensitive. Furthermore, previously established variations of lactoferrin [17] during this phase of lactation were confirmed via this method.

Following normalization as detailed, α-casein, β-casein, OPN, and CHRDL2 were examined in more detail to determine quantitative variations of specific phosphopeptides observed. These phosphoproteins were selected for quantitation because each analysis yielded identifiable phosphopeptides and a minimum of five non-phosphorylated peptides for normalization purposes. Quantitative variations in site occupancy of specific phosphopeptides and their standard deviations are annotated in Table 2. Two-tailed heteroscedastic Student's *t* tests were performed using the normalized

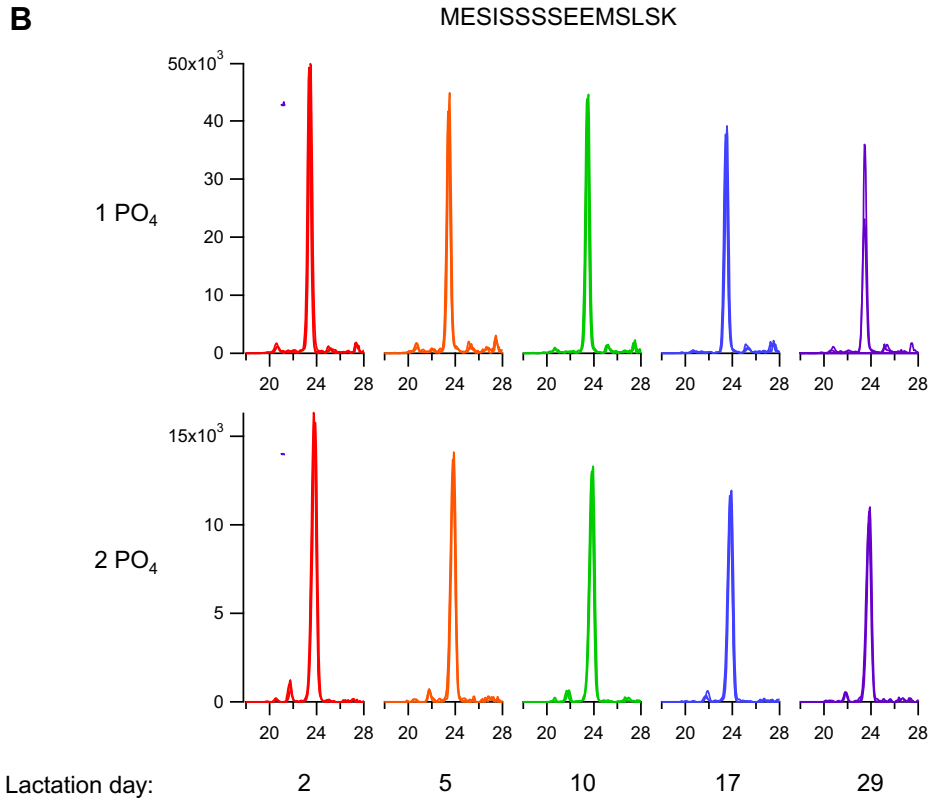

Fig.2. (B) Chromatograms corresponding to singly (top) and doubly (bottom) phosphorylated MESISSSSEEMSLSK peptide from α-casein are shown. A consistent, gradual decrease is observed for both the monophosphorylated and diphosphorylated peptides.

phosphopeptide intensities to determine the significance of the observed variations between different lactation days. The singly, doubly, and triply marked (asterisks) values correspond to $P < 0.05$, $P < 0.01$, and $P < 0.001$, respectively. The samples with the highest and lowest occupancies are also annotated. The experimentally determined phosphorylation sites are also indicated when applicable, but collision-induced dissociation (CID) fragmentation data were insufficient in several cases to unambiguously determine the sites of phosphorylation. The challenges of using CID for the determination of phosphorylation sites was well summarized in a recent study by Palumbo and Reid [18].

Changes in phosphorylation occupancy of β-casein

Isomeric structures of several phosphopeptides were also observed. For example, extracted ion chromatograms (EICs) corresponding to the monophosphorylated and diphosphorylated peptide ^{17}ETIESLSSSEESITEYK^{33} from β-casein are shown in Fig. 1. Triplicates of each EIC are overlaid to demonstrate the precision of both the peak intensities and the retention times. Notably, there are two resolved isomers of the monophosphorylated phosphopeptide and only one of the diphosphorylated analog. The presence of two isomers of the monophosphorylated ^{17}ETIESLSSSEESITEYK^{33} peptide suggests that there are two separate phosphorylation sites that may be phosphorylated initially. This is verified by careful examination of the MS/MS spectra of the monophosphorylated isomers. The preferred phosphorylation order has previously been shown to be Ser24 > Ser25 > Ser23 > Ser21 > Thr18 [12,19] using a combination of two-dimensional gels and MS/MS. Combining LC and MS/MS data in the current study suggests, however, that the phosphorylation is not strictly sequential and that the preference for the initial Ser24 and Ser25 phosphorylation is approximately 2:1. α-Casein is known to be phosphorylated by the mammary gland casein kinase (MGCK), which acts on amino acid sequences of (S/T)-X-(D/E/s/t). It is also possible that the strict phosphorylation order observed previously is followed and that the variation of the monophosphorylated isomer is due to differences in phosphatase expression during these time points. In this study, isoforms corresponding to zero, one, and two phosphates were observed. In certain instances, the sites of phosphorylation could be determined via CID.

Changes in phosphorylation occupancy of α-casein

In α-casein, phosphorylation sites are localized in two regions covered by two tryptic peptides. The quantitative behaviors of these two regions are shown separately in Fig. 2A and B. In each case, normalized EICs are overlaid in triplicate. Fig. 2A shows the behavior of the phosphopeptide ^{27}LQNPSESSEPIPLESR^{42}, with mono-, di-, and triphosphorylated versions of the peptide shown. Isomers are observed for the monophosphorylated form only. Despite little change in the total abundance of the predominant monophosphorylated form of this phosphopeptide, the isomer ratio varies from approximately 3:1 at day 2 to approximately 3:2 for all later time points. The diphosphorylated and triphosphorylated isoforms show no significant changes in abundance. The quantitative behavior of the ^{83}MESSISSSSEEMSLSK^{98} region of α-casein was also determined and is annotated in Table 2 along with the other phosphopeptides analyzed. This region has two potential primary phosphorylation sites for each of the MGCK and casein kinase II kinases. The exact sites of phosphorylation could not be definitively determined in this study, but a single isomer of the mono- and diphosphorylated versions of this peptide was observed. Previous work suggests that the primary phosphorylation occurs at Ser90 [13]. Minimal quantitative variations were observed.

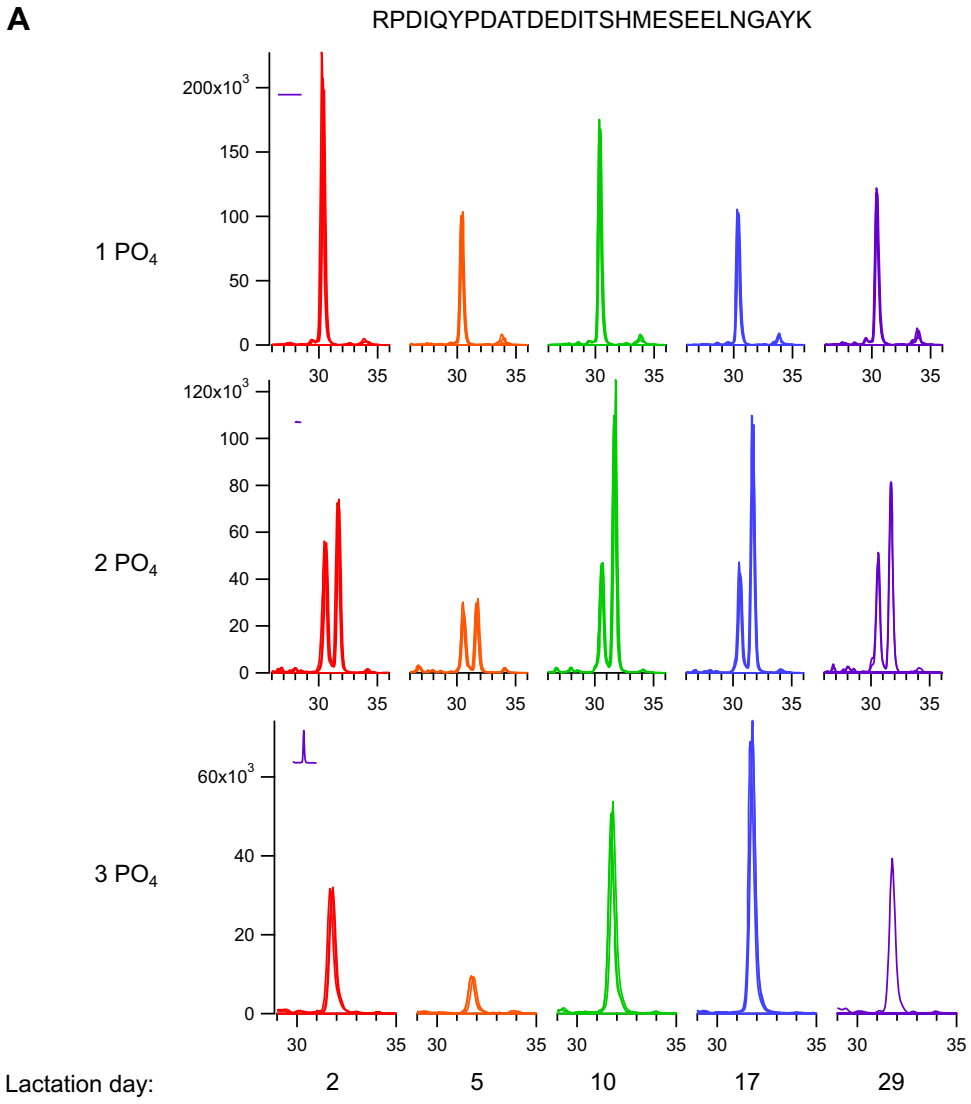

Fig.3. Overlaid triplicate EICs of three distinct regions of phosphorylation of OPN. (A) RPDIQYPDATDEDITSHMESEELNGAYK with one and two phosphates is examined. (B) corresponds to the C-terminal region FRISHELDSASSEVN, and panel C corresponds to ANDESNEHSDVIDSQELSK. For both panels A and B, the monophosphorylated peptides give a single isomer and highly dynamic occupancies, whereas the diphosphorylated peptides vary in disparate manners. (C) however, the monophosphopeptide has a single isomer, whereas the diphosphorylated form exhibits two isomers that vary similarly.

Changes in phosphorylation occupancy of OPN

OPN is an analytically challenging protein because it is extensively phosphorylated and glycosylated and contains a large region spanning approximately 35% of the protein sequence without a single tryptic cleavage site. Previous research has determined 2 N-glycosylation sites, 5 O-glycosylation sites, and 36 phosphorylation sites [20]. As shown in Fig. 3A, the peptide ^{176}RPDIQYPDATDEDITSHMESEELNGAYK^{203} is present in both mono- and diphosphorylated forms. Although the monophosphorylated form exhibits a single chromatographically resolved isomer, there are three for the diphosphorylated analog. Compellingly, the most abundant diphosphorylated isomer demonstrates a highly reproducible 4-fold difference between day 5 and day 10 of lactation. The second most abundant isomer shows a 2-fold difference between day 5 and day 2. There are four serine and threonine residues in this region, and three have been shown to be phosphorylated (Thr185, Ser191, and Ser195) [20]. For a diphosphorylated peptide with three possible phosphorylation sites, three isomers are expected, as verified by the presence of three chromatographic peaks. In this region, day 5 is the least occupied time point for both the mono- and diphosphorylated phosphoforms.

Compellingly, the separate regions of OPN demonstrate disparate changes in phosphorylation occupancy. Fig. 3B shows the normalized EICs of the C-terminal phosphopeptide ^{300}FRISHELDSASSEVN^{314}. Mono- and diphosphorylated analogs were observed for this region as well, and in each case day 17 was the least occupied time point. Between day 17 and day 29, 3- to 4-fold occupancy differences were observed. Another peptide, ^{250}ANDESNEHSDVIDSQELSK^{268}, displays a similar phosphorylation pattern, yet observed changes in this region of OPN were only 2-fold, as seen in Fig. 3C. The remaining OPN regions that were quantified are summarized in Table 2. There appears to be very little change in the overall phosphorylation of OPN on the whole, yet significant changes for many of the sites were observed.

Discussion

Tracking relative changes in protein phosphorylation of milk proteins is especially difficult because the protein amounts are

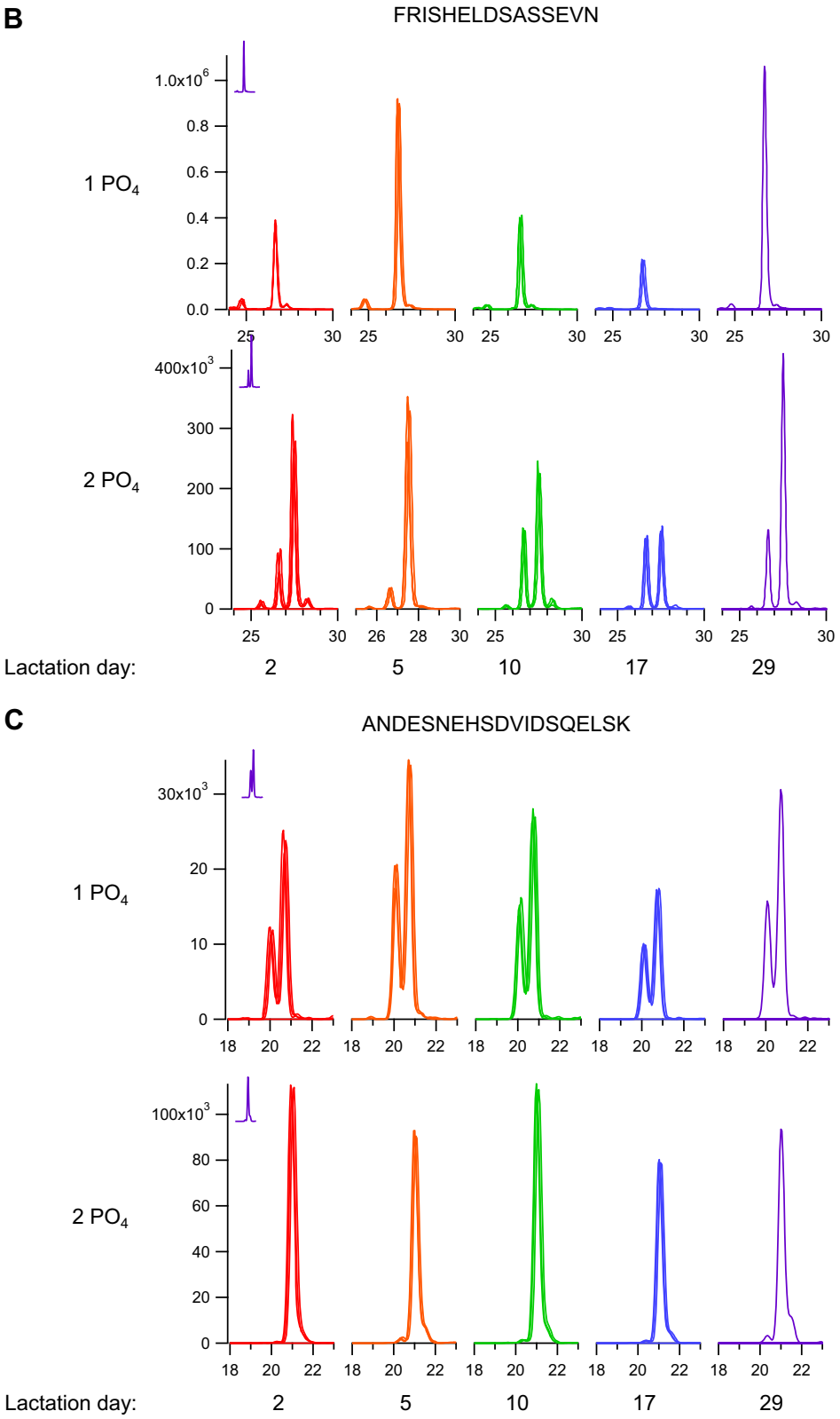

Fig. 3 (*continued*)

known to vary during lactation. Therefore, a normalization scheme was implemented to correct for changes in protein expression. The total peptide intensity from each protein was used as a proxy for changes in protein expression. The CVs for this method after three replicate analyses were comparable to those in quantitation studies that use isotopically labeled peptides; however, this method has an advantage in that it does not require expensive isotopic labeling reagents, unlike the SILAC (stable isotope labeling by amino acids in cell culture) [21] and ICAT (isotope-coded affinity tags) [22] approaches. Another advantage of using a peptide-level nor-

malization strategy is accounting for potential differences in digestion efficiency between samples. Despite the best efforts to achieve a reproducible digestion, there is always potential for variation in the digestion efficiency. A peptide-level normalization accounts for this variation because peptides and phosphopeptides are generated simultaneously. The reproducibility afforded by this method is likely a combination of automating the enrichment process and minimizing sample handling.

As expected, the normalization scheme mainly decreased the magnitude of the observed changes in protein phosphorylation (Supplementary Fig. 2 in supplementary material); thus, omitting the normalization would have overestimated the relative changes in phosphorylation. This result has implications for other label-free phosphorylation quantification approaches. If determination of the relative amount of site occupancy is the goal, then variations of both protein quantity and digestion efficiency between samples must be taken into consideration. The normalization scheme developed accounts for both of these changes. The precision of these measurements is also comparable to that in the other quantitative approaches, with 46% of all quantified phosphopeptides having less than 10% CVs and 85% having less than 30% CVs in this study.

It should be noted that the results of this study are preliminary because the samples were provided by a single individual. A larger study must be performed before generalizations may be made regarding quantitative changes of milk phosphorylation in the population. This study does, however, suggest that human milk is an interesting target for future experiments and presents an effective methodology to carry out those experiments. Possible biological implications of this work are discussed below.

Although there were changes in total protein phosphorylation during lactation for some phosphoproteins, in other instances there was very little protein-level phosphorylation variation. OPN is extensively phosphorylated, and the sites vary in occupancy to such a degree that one might expect significant protein-level variation. Instead, individual phosphorylation sites were either up- or down-regulated in a contrary manner to effect substantial local phosphorylation variation but little change in the overall phosphorylation of OPN. Little data exist to determine any potential changes in the function among the hundreds of possible phosphoforms of this protein; therefore, the functional implications of these changes are unknown. OPN research to date has shown that it is a multifunctional protein implicated in cell migration, mineralization, cellular proliferation, and osteoblast formation [23–29]. OPN has been shown to exhibit both pro- and anti-inflammatory functions depending on the location in the body [24]. Therefore, it is possible that the role of OPN also changes during the course of lactation; the change could be mediated by dynamic phosphorylation. Given the many biological functions that OPN possesses throughout the body and the extent of phosphorylation present on the protein, phosphorylation likely regulates function to a large extent.

Because our approach used a bottom-up approach, changes in OPN phosphorylation were localized to individual phosphopeptides containing up to three phosphorylation sites; therefore changes in individual regions were identifiable. With a protein that is as extensively phosphorylated as OPN, a top-down analytical method would have greatly complicated elucidation of the site-specific dynamic phosphorylation observed.

The phosphorylation sites of α-casein are localized on two separate tryptic peptides. One of these regions shows little to no variation in the samples analyzed in this study, and the other one demonstrates quantitative variations of up to 2-fold. One might expect that this would show a significant change in the overall phosphorylation intensity as measured by MS. However, the intensity of the variable phosphopeptides is approximately an order of magnitude lower than that of the phosphopeptides that are unchanging, and subsequently no significant protein-level differences are observed. A previous study suggested that the difference in intensity between the two phosphorylation regions results from a site occupation difference between these regions rather than differences in ionization efficiency [13].

Although the determination of the relative quantitative differences in phosphorylation occupancy was the primary goal of this study, identification of previously unreported phosphorylation sites was also achieved. In addition to the known phosphoproteins discussed previously, minor phosphorylation was also detected on α-lactalbumin, a highly abundant whey protein, in this study. The phosphorylation sites detected in these analyses, Ser95 and Thr105, are consistent with the known specificity of MGCK. Because MGCK is the most active kinase in the mammary gland, and considering that α-lactalbumin possesses the known motif required, it is likely that the trace level of phosphorylation detected here is carried out by the MGCK. In addition, bovine α-lactalbumin is phosphorylated by the casein kinase [30]. This is the first known report of enzymatic phosphorylation of this abundant human whey protein. Functionally, α-lactalbumin is known to modulate the specificity of the β-1,4-galactosyltransferase to enable the production of lactose in the mammary epithelial cells. β-1,4-Galactosyl transferase was also identified as phosphorylated in this study. α-Lactalbumin can also induce cellular apoptosis on formation of a complex with fatty acids during digestion [31].

This is the first report of the characterization of CHRDL2 phosphorylation in human milk. Interestingly, CHRDL2 possesses three von Willebrand factor type C repeats, suggesting that it is potentially secreted as a multiprotein complex. Regardless of secretion state, CHRDL2 has been implicated in several biological processes, including myoblast and osteoblast maturation, bone morphogenic protein inhibition, and tumor angiogenesis [32]. CHRDL2 is known to be highly expressed in tumors and epithelial cells [33]. Its role in both milk and the normal mammary gland, however, is unreported to date.

Conclusions

In this study, a label-free LC–MS/MS quantification method was applied to the study of human milk phosphorylation from an individual during the first month of lactation. This is the first known report of relative quantitation of human milk proteins during lactation. Because the expression levels of milk proteins are known to vary during the course of lactation, a normalization strategy based on total peptide signal was developed and incorporated into the quantitative method to elucidate changes in phosphorylation site occupancy. The precision of the results obtained in this study is comparable to that in published results using expensive isotopic labeling reagents.

Very few studies have been performed to elucidate the phosphoproteome of human milk, and substantial work remains to expand our understanding of milk protein phosphorylation to include low-abundance phosphoproteins. The abundant caseins and OPN are the best characterized phosphoproteins to date. This is the first known report of α-lactalbumin phosphorylation, a highly abundant and well-studied whey protein, yet the trace levels of phosphorylation identified were previously unknown. In addition, this is the first known study to characterize CHRDL2 phosphorylation in human milk.

Although this approach did not use many of the protein fractionation strategies that site-directed phosphoproteomic studies employ, novel sites of phosphorylation were nevertheless determined for a few milk proteins. A more extensive sample fractionation would likely facilitate the identification of additional novel phosphorylation sites in human milk proteins. However, extensive

sample fractionation would also complicate the quantitative determination of phosphorylation occupancy as determined in this study.

In addition, it should be noted that the enrichment strategy used has been shown to bias the phosphopeptides observed. Titanium dioxide has been shown to preferentially enrich for singly phosphorylated phosphopeptides and serine and threonine phosphorylated phosphopeptides [34]. Other enrichment strategies have their biases as well. Phosphotyrosine antibodies are specific to phosphotyrosine residues, which is critical because these residues are much lower in abundance than phosphoserine or phosphothreonine residues. In addition, immobilized metal affinity chromatography has a higher affinity to multiply phosphorylated phosphopeptides [34]. Future work must consider the enrichment strategy to be a vital component of the research plan because it will influence the information gained. For example, human milk proteins are extensively phosphorylated on serine and threonine residues, and a different strategy would be required to characterize phosphotyrosine-containing peptides.

Although many phosphopeptides demonstrate dynamic occupancy rates during the first month of lactation, it is unclear at this time what the observed changes may signify biologically. Continuing this study with a larger cohort will lead to a better understanding as to the extent of quantitative changes in the population at large. The existence of dynamic phosphorylation in early lactation potentially represents a biological adjustment to meet the needs of the infant. Understanding how these specific components change during lactation may lend critical insight to early infant development.

Appendix A. Supplementary data

Supplementary data associated with this article can be found, in the online version, at doi:10.1016/j.ab.2010.08.031.

References

[1] S. Mohammed, K. Kraiczek, M.W. Pinkse, S. Lemeer, J.J. Benschop, A.J. Heck, Chip-based enrichment and nanoLC–MS/MS analysis of phosphopeptides from whole lysates, J. Proteome Res. 7 (2008) 1565–1571.
[2] G. Boehm, B. Stahl, Oligosaccharides from milk, J. Nutr. 137 (suppl. 2) (2007) 847S–849S.
[3] B. Lonnerdal, Nutritional and physiologic significance of human milk proteins, Am. J. Clin. Nutr. 77 (2003) 1537S–1543S.
[4] D.R. Hendrixson, J. Qiu, S.C. Shewry, D.L. Fink, S. Petty, E.N. Baker, A.G. Plaut, J.W.St. Geme 3rd, Human milk lactoferrin is a serine protease that cleaves *Haemophilus* surface proteins at arginine-rich sites, Mol. Microbiol. 47 (2003) 607–617.
[5] T. Olivecrona, O. Hernell, Human milk lipases and their possible role in fat digestion, Padiatr. Padol. 11 (1976) 600–604.
[6] G. Picariello, P. Ferranti, O. Fierro, G. Mamone, S. Caira, A. Di Luccia, S. Monica, F. Addeo, Peptides surviving the simulated gastrointestinal digestion of milk proteins: biological and toxicological implications, J. Chromatogr. B 878 (2010) 295–308.
[7] B. Lonnerdal, Breast milk: a truly functional food, Nutrition 16 (2000) 509–511.
[8] R.E. Ward, M. Ninonuevo, D.A. Mills, C.B. Lebrilla, J.B. German, In vitro fermentation of breast milk oligosaccharides by *Bifidobacterium infantis* and *Lactobacillus gasseri*, Appl. Environ. Microbiol. 72 (2006) 4497–4499.
[9] L.A. Hanson, M. Korotkova, E. Telemo, Breast-feeding, infant formulas, and the immune system, Ann. Allergy Asthma Immunol. 90 (2003) (Suppl. 3) (2003) 59–63.
[10] E.B. Isaacs, B.R. Fischl, B.T. Quinn, W.K. Chong, D.G. Gadian, A. Lucas, Impact of breast milk on IQ, brain size, and white matter development, Pediatr. Res. 67 (2010) 357–362.
[11] C. Kunz, B. Lonnerdal, Re-evaluation of the whey protein/casein ratio of human milk, Acta Paediatrica 81 (1992) 107–112.
[12] A.G. Poth, H.C. Deeth, P.F. Alewood, J.W. Holland, Analysis of the human casein phosphoproteome by 2-D electrophoresis and MALDI–TOF/TOF MS reveals new phosphoforms, J. Proteome Res. 7 (2008) 5017–5027.
[13] F. Kjeldsen, M.M. Savitski, M.L. Nielsen, L. Shi, R.A. Zubarev, On studying protein phosphorylation patterns using bottom-up LC–MS/MS: the case of human α-casein, Analyst 132 (2007) 768–776.
[14] E.S. Sorensen, L. Moller, M. Vinther, T.E. Petersen, L.K. Rasmussen, The phosphorylation pattern of human α_{s1}-casein is markedly different from the ruminant species, Eur. J. Biochem. 270 (2003) 3651–3655.
[15] W. Zhou, M.M. Ross, A. Tessitore, D. Ornstein, A. Vanmeter, L.A. Liotta, E.F. Petricoin 3rd, An initial characterization of the serum phosphoproteome, J. Proteome Res. 8 (2009) 5523–5531.
[16] W.M. Old, K. Meyer-Arendt, L. Aveline-Wolf, K.G. Pierce, A. Mendoza, J.R. Sevinsky, K.A. Resing, N.G. Ahn, Comparison of label-free methods for quantifying human proteins by shotgun proteomics, Mol. Cell. Proteomics 4 (2005) 1487–1502.
[17] Y. Hirai, N. Kawakata, K. Satoh, Y. Ikeda, S. Hisayasu, H. Orimo, Y. Yoshino, Concentrations of lactoferrin and iron in human milk at different stages of lactation, J. Nutr. Sci. Vitaminol. (Tokyo) 36 (1990) 531–544.
[18] A.M. Palumbo, G.E. Reid, Evaluation of gas-phase rearrangement and competing fragmentation reactions on protein phosphorylation site assignment using collision induced dissociation–MS/MS and MS^3, Anal. Chem. 80 (2008) 9735–9747.
[19] R. Greenberg, M.L. Groves, H.J. Dower, Human β-casein: amino acid sequence and identification of phosphorylation sites, J. Biol. Chem. 259 (1984) 5132–5138.
[20] B. Christensen, M.S. Nielsen, K.F. Haselmann, T.E. Petersen, E.S. Sorensen, Post-translationally modified residues of native human osteopontin are located in clusters: Identification of 36 phosphorylation and five O-glycosylation sites and their biological implications, Biochem. J. 390 (2005) 285–292.
[21] S.E. Ong, B. Blagoev, I. Kratchmarova, D.B. Kristensen, H. Steen, A. Pandey, M. Mann, Stable isotope labeling by amino acids in cell culture, SILAC, as a simple and accurate approach to expression proteomics, Mol. Cell. Proteomics 1 (2002) 376–386.
[22] S.P. Gygi, B. Rist, S.A. Gerber, F. Turecek, M.H. Gelb, R. Aebersold, Quantitative analysis of complex protein mixtures using isotope-coded affinity tags, Nat. Biotechnol. 17 (1999) 994–999.
[23] G. Chakraborty, S. Jain, R. Behera, M. Ahmed, P. Sharma, V. Kumar, G.C. Kundu, The multifaceted roles of osteopontin in cell signaling, tumor progression, and angiogenesis, Curr. Mol. Med. 6 (2006) 819–830.
[24] H.J. Cho, H.S. Kim, Osteopontin: a multifunctional protein at the crossroads of inflammation, atherosclerosis, and vascular calcification, Curr. Atheroscler. Rep. 11 (2009) 206–213.
[25] T. Standal, M. Borset, A. Sundan, Role of osteopontin in adhesion, migration, cell survival, and bone remodeling, Exp. Oncol. 26 (2004) 179–184.
[26] J. Sodek, A.P. Batista da Silva, R. Zohar, Osteopontin and mucosal protection, J. Dent. Res. 85 (2006) 404–415.
[27] J. Agnholt, J. Kelsen, L. Schack, C.L. Hvas, J.F. Dahlerup, E.S. Sorensen, Osteopontin, a protein with cytokine-like properties, is associated with inflammation in Crohn's disease, Scand. J. Immunol. 65 (2007) 453–460.
[28] S.K. Ramaiah, S. Rittling, Pathophysiological role of osteopontin in hepatic inflammation, toxicity, and cancer, Toxicol. Sci. 103 (2008) 4–13.
[29] K.X. Wang, D.T. Denhardt, Osteopontin: role in immune regulation and stress responses, Cytokine Growth Factor Rev. 19 (2008) 333–345.
[30] E.W. Bingham, N. Parris, H.M. Farrell Jr., Phosphorylation of β-casein and α-lactalbumin by casein kinase from lactating bovine mammary gland, J. Dairy Sci. 71 (1988) 324–336.
[31] M. Svensson, A. Hakansson, A.K. Mossberg, S. Linse, C. Svanborg, Conversion of α-lactalbumin to a protein inducing apoptosis, Proc. Natl. Acad. Sci. USA 97 (2000) 4221–4226.
[32] A. Oren, A. Toporik, S. Biton, N. Almogy, D. Eshel, J. Bernstein, K. Savitsky, G. Rotman, HCHL2, A novel chordin-related gene, displays differential expression and complex alternative splicing in human tissues and during myoblast and osteoblast maturation, Gene 331 (2004) 17–31.
[33] I. Wu, M.A. Moses, BNF-1, a novel gene encoding a putative extracellular matrix protein, is overexpressed in tumor tissues, Gene 311 (2003) 105–110.
[34] N. Sugiyama, T. Masuda, K. Shinoda, A. Nakamura, M. Tomita, Y. Ishihama, Phosphopeptide enrichment by aliphatic hydroxy acid-modified metal oxide chromatography for nano-LC–MS/MS in proteomics applications, Mol. Cell. Proteomics 6 (2007) 1103–1109.